Proceedings of the 17th World Congress
The International Federation of Automatic Control
Seoul, Korea, July 6-11, 2008

Performance Improvement in Unfalsified Control Using Neural Networks

Jinhua Cao * **Margareta Stefanovic** **

* *Dept. of Electrical and Computer Engineering, University of Wyoming, Laramie, WY, 82071 USA (e-mail: jcao@ uwyo.edu).*
** *Dept. of Electrical and Computer Engineering, University of Wyoming, Laramie, WY, 82071 USA (Tel: 307-766-6780; e-mail: mstefano@uwyo.edu)*

Abstract: In this paper, a novel combination of unfalsified control and intelligent control is proposed to improve the dynamic performance of an uncertain system. A PID controller, whose parameters are adaptively tuned by switching among members of a given candidate set using observed plant data, is presented and compared with multi-model adaptive control. Two different cost functions are compared for their capability in selecting the "best" controller. The principle of Radial Basis Function Neural Networks (RBFNN) is used to update the parameters of the selected PID controller to further improve the performance. Simulation results demonstrate that the proposed control switching strategy compares favorably to the alternatives.

Keywords: Neural networks; unfalsified control; PID control; dynamic performance.

1. INTRODUCTION

To address the emerging need for robustness of adaptive systems towards larger uncertainties or to achieve tighter performance specifications, several recent important advances have involved multi-model controller switching formulations of the adaptive control problem, *e.g.* supervisory based control design in Balakrishnan and Narendra [1994, 1997], or data-driven unfalsified adaptive control methods of Tsao and Safonov [1997], which exploit evidence in the plant output data to switch a controller out of the loop when the evidence proves that the controller is failing to achieve the stated goal. These formulations have led to improved optimization-based adaptive control theories and, most importantly, significantly weaker assumptions of prior knowledge.

In contrast to the indirect, estimator-based multi-model adaptive control schemes (Balakrishnan and Narendra [1997], Chen and Narendra [2001]), unfalsified control is an approach based on direct controller performance (Tsao and Safonov [1997], Stefanovic and Safonov [2006], Stefanovic et al. [2004], Wang et al. [2004]). It does not attempt to make assumptions about the plant in order to deduce overall switched system stability. Thus, the potential problem of a 'model-mismatch" instability related to the multi-model based adaptive schemes can be avoided. Of course, plant models still play an important role in the design of the candidate controller set.

Recently, other approaches have been employed in extending multi-model adaptive control to the modeling and control of more complex, unknown, time-varying dynamic systems, such as fuzzy control (Skrjanc et al. [2003]) and Neural Networks (NN) control (Chen and Narendra [2001], Zhai and Fei [2005]). Neural networks are powerful tools for approximating unknown nonlinear functions, which extends their application to the control of unknown, nonlinear dynamic systems. In Lim and Lewis [1999], results on stability of the neural networks have been obtained. In Chen and Narendra [2001], some results about the signal boundedness using neural networks in adaptive control have been established.

To our knowledge, unfalsified control has not been examined in the combination with the neural network schemes. In this paper, we propose new results on the performance improvement in Multiple Controller Adaptive Control (MCAC) systems by using Neural Networks. Also reported is the comparison between the obtained results and the performance improvement in Multiple Model Adaptive Control schemes using neural networks.

The paper is organized as follows. In Section 2, the formulation of unfalsified control problem is reviewed. In Section 3, main results on stability of the switched data-driven multi-controller adaptive control problem are reviewed. In Section 4, a Radial Basis Function Neural Networks(RBFNN) algorithm is stated and used in the unfalsified (data-driven) control problem. Simulations are conducted and discussed in Section 5. Concluding remarks are provided in Section 6.

2. UNFALSIFIED CONTROL PROBLEM

The multiple controller unfalsified switching system is described below, utilizing a set of candidate PID controllers, which is one of the most widely used methods in the industry. In Jun and Safonov [1999], fundamentals of the unfalsified control theory and its use in conjunction with

PID controllers are described. To apply this approach, one first constructs a bank of PID controllers. Then, the fictitious reference signal and fictitious error signal for individual PID controllers are generated. Given the fictitious reference signal, plant input signal, and plant output signal, the "best" controller is selected from the candidate set using a properly designed cost criterion.

Fictitious Reference Signal. According to Jun and Safonov [1999], the PID controller is written as:

$$u = (k_p + \frac{k_I}{s})(r - y) - \frac{sk_D}{\varepsilon s+1}y$$

where ε is a small number, added to approximate the derivative part. Hence, the fictitious reference signal for the candidate controller with the index i can be calculated as:

$$\widetilde{r_i} = y + \frac{s}{sk_{P_i}+k_{I_i}}(u + \frac{sk_{D_i}}{\varepsilon s+1}y)$$

The fictitious error signal for the candidate controller i (defined as the error between its fictitious reference signal and the actual plant output), is given as:

$$\widetilde{e_i} = \widetilde{r_i} - y$$

Cost Function. An important step in the unfalsified control is to design a suitable cost function to adjust controller parameters based on the measured data alone. First, we consider the cost function proposed in the Jun and Safonov [1999]:

$$J_i(t) = -\rho + \int_0^t \Gamma_{spec}(\widetilde{r_i}(t), y(t), u(t))dt \qquad (1)$$

where $\rho > 0$ is used to judge whether a certain controller is falsified or not, and Γ_{spec} is chosen as

$$\Gamma_{spec}(\widetilde{r_i}(t), y(t), u(t)) = (w_1 * (\widetilde{r_i}(t) - y(t))^2 + (w_2 * u(t))^2 - \sigma^2 - \widetilde{r_i}(t)^2$$

where w_1 and w_2 are weighting filters chosen by the designer, and σ is a constant representing the r.m.s. effects of noise on the cost. In Stefanovic and Safonov [2006], the cost function above was shown to be non-cost-detectable, and therefore, it may, in some cases, discard the stabilizing controller, and latch onto a destabilizing one.

3. SWITCHED SYSTEM STABILITY

Recall the results on stability in a multi-controller unfalsified setting. Consider the system $\Sigma : \mathfrak{L}_{2e} \longrightarrow \mathfrak{L}_{2e}$.

Definition 1. Stability of the system $\Sigma : \boldsymbol{w} \mapsto \boldsymbol{z}$ is said to be *unfalsified* by the data $(\boldsymbol{w}, \boldsymbol{z})$ if there exist $\beta, \alpha \geq 0$ such that the following holds:

$$||\boldsymbol{z}||_\tau < \beta||\boldsymbol{w}||_\tau + \alpha, \forall \tau > 0; \qquad (2)$$

Otherwise, we say that stability of the system Σ is *falsified* by $(\boldsymbol{w}, \boldsymbol{z})$.

Consider the cost minimization hysteresis switching algorithm reported in Morse et al. [1992], together with the cost functional $J(K, z, t)$. The algorithm returns, at each time t, a controller $\hat{K}_t$ which is the active controller in the loop:

ε-hysteresis switching algorithm A1

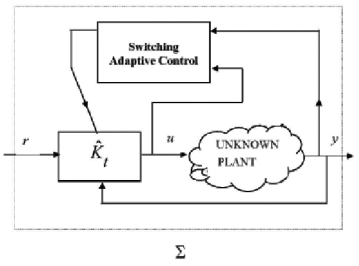

Fig. 1. Switching adaptive control system $\Sigma(\hat{K}_t, P)$.

Morse et al. [1992]

$$\hat{K}_t = \arg\min_{K \in \mathbf{K}}\{J(K, z, t) - \varepsilon\delta_{K\hat{K}_{t^-}}\}$$

where δ_{ij} is the Kronecker's δ, and t^- is the limit of τ from below as $t \longrightarrow \tau$.

The switch occurs only when the current unfalsified cost related to the currently active controller exceeds the minimum (over the finite set of candidate controllers $\mathbf{K}$) of the current unfalsified cost by at least ε. The hysteresis step ε serves to limit the number of switches on any finite time interval to a finite number, and so prevents the possibility of the limit cycle type of instability. It also ensures a non-zero dwell time between switches.

Definition 2. (Stefanovic and Safonov [2006]) Let r denote the input and $z_d = \Sigma(\hat{K}_t, \mathcal{P})r$ denote the resulting plant data collected while $\hat{K}_t$ is in the loop. Consider the adaptive control system $\Sigma(\hat{K}_t, \mathcal{P})$ of Fig. 1 with input r and output z_d. The pair $(J, \mathbf{K})$ is said to be *cost detectable* if, without any assumption on the plant P and for every $\hat{K}_t \in \mathbf{K}$ with finitely many switching times, the following statements are equivalent:

(1) $J(K_N, z_d, t)$ is bounded as t increases to infinity.
(2) Stability of the system $\Sigma(\hat{K}_t, \mathcal{P})$ is unfalsified by the input-output pair (r, z_d).

Definition 3. The adaptive control problem is said to be *feasible* if a candidate controller set $\mathbf{K}$ contains at least one controller such that the system $\Sigma(K, \mathcal{P})$ is stable. A controller $K \in \mathbf{K}$ is said to be a *feasible controller* if the system $\Sigma(K, \mathcal{P})$ is stable.

Theorem 4. (Stefanovic and Safonov [2006]) Consider the feedback adaptive control system Σ in Fig. 1, together with the hysteresis switching algorithm A1. Suppose the following holds: the adaptive control problem is feasible, the associated cost functional $J(K, z, t)$ is monotone in time, the pair $(J, \mathbf{K})$ is cost detectable, and the candidate controllers have stable causal left inverses. Then, the switched closed-loop system is stable. In addition, for each z, the system converges after finitely many switches to the controller K_N that satisfies the performance inequality

$$J(K_N, z, \tau) \leq J_{true}(K_{RSP}) + \epsilon \quad \text{for all } \tau. \qquad (3)$$

3.1 Cost Function Example

An example of the cost function and the conditions that ensure stability and finiteness of switches according to Theorem 4 may be constructed as follows. Consider (a not necessarily zero-input zero-output) system $\Sigma : \mathfrak{L}_{2e} \rightarrow \mathfrak{L}_{2e}$ in Fig. 1. Choose as a cost functional:

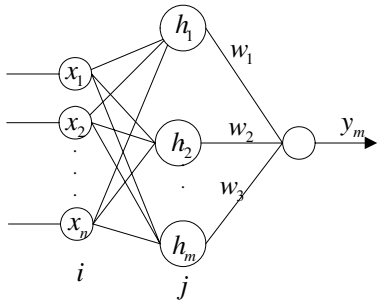

Fig. 2. RBF Neural Network Structure.

$$J(K,z,t)=\max_{\tau\le t}\frac{||y||_\tau^2+||u||_\tau^2}{||\tilde{r}_K||_\tau^2+\alpha} \tag{4}$$

where α is an arbitrary positive number, used to prevent division by zero when $\tilde{r}=y=u=0$ (unless Σ has zero-input zero-output property). Alternatively, in order to avoid the restriction to the minimum phase (stably causally left invertible) controllers (which would assure the causality and incremental stability of the map $[u,y]\to\tilde{r}$), the denominator of (4) can contain $\tilde{v}_K$ instead of $\tilde{r}_K$ (Manuelli et al. [2007], Dehghani et al. [2007], where $\tilde{v}_K$ is defined via the matrix fraction description (MFD) of the controller K, as $K=D_K^{-1}N_K$ and $\tilde{v}_K(t)=(-N_K)(-y(t))+D_Ku(t)$.

$$J(K,z,t)=\max_{\tau\le t}\frac{||y||_\tau^2+||u||_\tau^2}{||\tilde{v}_K||_\tau^2+\alpha} \tag{5}$$

Both (4) and (5) have been shown to satisfy the required properties of Theorem 4. Stability verification for (4) and (5) is provided in Stefanovic and Safonov [2006]. The results of Manuelli et al. [2007] also ensure 'internal stability' of the adaptive system designed using cost-detectable cost-functions of the forms (4) or (5).

4. THE USE OF NEURAL NETWORK

The conventional PID controllers with fixed parameters may deteriorate the control performance in accordance with the complexity of the plant. In this section, we attempt to select the best suitable PID controller using the switching algorithm A1 and the cost function (4), combined with the use of a three-layer RBFNN, as shown in Fig. 2, to adaptively update its parameters to achieve a better performance.

In the RBFNN, $X=[x_1,x_2,...x_n]^T$ denotes the input vector. Assume the radial basis vector is $H=[h_1,h_2,...h_j,...h_m]^T$, where h_j is the Gaussian function:

$$h_j=\exp\left(-\frac{\|X-C_j\|^2}{2b_j^2}\right)\ (j=1,2,...,m)$$

and $C_j=[c_{j1},c_{j2},...c_{ji},...,c_{jn}]^T$ is the center vector of the jth node.

Let $B=[b_1,b_2,...,b_m]^T$, where $b_j>0$ is the basis width of the jth node; $W=[w_1,w_2,...,w_j,...w_m]^T$ is the weight vector. As shown in Fig. 2, the NN output is

$$y_m=\sum_{j=1}^{m}w_jh_j$$

The RBFNN identification performance index is

$$E=\tfrac{1}{2}(y(k)-y_m(k))^2$$

Then, according to gradient descent algorithm, the output weights, node centers, and basis width parameters are calculated as follows:

$$\Delta w_j=\frac{\partial E}{\partial w_j}=(y(k)-y_m(k))h_j$$

$$w_j(k)=w_j(k-1)+\eta\Delta w_j+\alpha(w_j(k-1)-w_j(k-2))$$

$$\Delta b_j=\frac{\partial E}{\partial b_j}=(y(k)-y_m(k))w_jh_j\frac{\|X-C_j\|^2}{b_j^3}$$

$$b_j(k)=b_j(k-1)+\eta\Delta b_j+\alpha(b_j(k-1)-b_j(k-2))$$

$$\Delta c_{ji}=\frac{\partial E}{\partial c_j}=(y(k)-y_m(k))w_jh_j\frac{x-c_{ji}}{b_j^2}$$

$$c_{ji}(k)=c_{ji}(k-1)+\eta\Delta c_{ji}+\alpha(c_{ji}(k-1)-c_{ji}(k-2))$$

where η is the learning rate, α is the momentum factor.

In this paper, the inputs of the RBFNN identification is chosen as

$$x_1=\Delta u(k)=u(k)-u(k-1)$$
$$x_2=y(k)$$
$$x_3=y(k-1)$$

The Jacobian Algorithm, used in the sequel, is:

$$\frac{\partial y(k)}{\partial\Delta u(k)}\approx\frac{\partial y_m(k)}{\partial\Delta u(k)}=\sum_{j=1}^{k}w_jh_j\frac{c_{ji}-\Delta u(k)}{b_j^2}$$

Here, we use this algorithm to update the PID controller parameters, selected by the above unfalsified control switching algorithm A1. Assume the remaining error of the unfalsified control is

$$error(k)=r-y(k)$$

Hence, the inputs of the RBFNN based PID controller are

$$error\_p=error(k)-error(k-1)$$
$$error\_i=error(k)$$
$$error\_d=error(k)-2error(k-1)+error(k-2)$$

The control algorithm is given as:

$$u(k)=u(k-1)+\Delta u(k)$$

$$\Delta u(k)=k_p(error(k)-error(k-1))+k_i(error(k))+k_d(error(k)-2error(k-1)+error(k-2))$$

Here, the NN approximation index is

$$E(k)=\tfrac{1}{2}error(k)^2$$

where k_p,k_i,k_d are adjusted by the gradient descent algorithm:

$$\Delta k_p=-\eta\frac{\partial E}{\partial k_p}=-\eta\frac{\partial E}{\partial y}\frac{\partial y}{\partial\Delta u}\frac{\partial\Delta u}{\partial k_p}=\eta error(k)\frac{\partial y}{\partial\Delta u}error\_p$$

$$\Delta k_i=-\eta\frac{\partial E}{\partial k_i}=-\eta\frac{\partial E}{\partial y}\frac{\partial y}{\partial\Delta u}\frac{\partial\Delta u}{\partial k_i}=\eta error(k)\frac{\partial y}{\partial\Delta u}error\_i$$

$$\Delta k_d=-\eta\frac{\partial E}{\partial k_d}=-\eta\frac{\partial E}{\partial y}\frac{\partial y}{\partial\Delta u}\frac{\partial\Delta u}{\partial k_d}=\eta error(k)\frac{\partial y}{\partial\Delta u}error\_d$$

where $\frac{\partial y}{\partial\Delta u}$ is the plant Jacobian, which is calculated by the RBFNN.

The control structure is shown in Fig. 3.

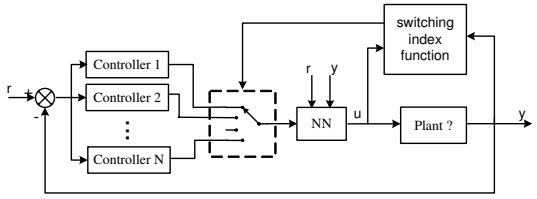

Fig. 3. Unfalsified Control Using NN.

According to Jun and Safonov [1999], when a new controller is selected, the control algorithm resets the states of the integrator term, and the approximate differentiator term (to prevent the discontinuity). Thus, the whole algorithm can be presented as follows. The data u and y are measured; $\widetilde{r_i}$ and $\widetilde{e_i}$ are calculated from the candidate controller and measured plant data; J_i is calculated, and the controller $\arg\min_{1\le i\le N} J_i(t)$ is switched into the loop; at the switching times, the controller states are reset; the RBFNN is combined to the selected controller to update the PID parameters. Theoretical validation of the stability of the unfalsified control system is described in Stefanovic and Safonov [2006] (see Section 2). The combination of NN in unfalsified control does not alter the stability of the switched system. Once the RBFNN is combined with the selected controller, the switched controller remains in the candidate controller set, in which all controllers are "supervised" by the switching law. When the measured data start revealing instability, the currently active controller is quickly switched out of the loop and replaced by another one. Hence, stability of the overall switched unfalsified control system combined with the neural networks is preserved (under the feasibility assumption).

5. SIMULATIONS AND DISCUSSION

This section presents simulation results with no disturbance, no noise, and zero-initial conditions, though this can be relaxed.

To illustrate the algorithm described above and compare with the simulation results of multiple-model adaptive control in Balakrishnan and Narendra [1994], we have reproduced the same simulation setting as in Balakrishnan and Narendra [1994]. The transfer function of the actual plant (unknown from the control perspective) is assumed to be:

$$G_p(s) = \frac{a}{s^2+bs+c}$$

The parameters a, b, c are assumed to lie in the compact set given by $S = \{0.5 \le a \le 2, -0.6 \le b \le 3.4, -2 \le c \le 2\}$. The reference input is a square wave signal with unit amplitude and period 10 seconds, and the reference model, whose output is to be tracked, is taken as $W_m(s) = \frac{1}{s^2+1.4s+1}$. Simulations were conducted on three plants found in Balakrishnan and Narendra [1994], all unstable oscillatory plants: $0.5/(s^2-0.35s+2)$, $0.5/(s^2-0.5s+2)$, $0.5/(s^2+0.5s-2)$.

Simulation 1 : Here we demonstrate that the cost-detectable cost function is "safer" than the non-cost-detectable one. In this case, the controller set is taken as $K_P = \{1, 5, 20, 50, 100\}$, $K_I = \{1, 5, 20, 30, 50, 100\}$, $K_D = \{0.2, 0.5, 1, 5, 15\}$. The simulation results are shown

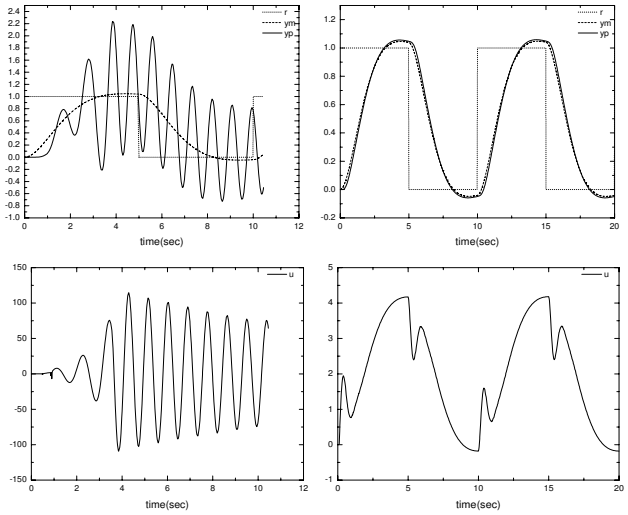

(a) (b)

Fig. 4. I/O data for unstable oscillatory plant $G_p(s) = 0.5/(s^2-0.35s+2)$ with two different cost functions

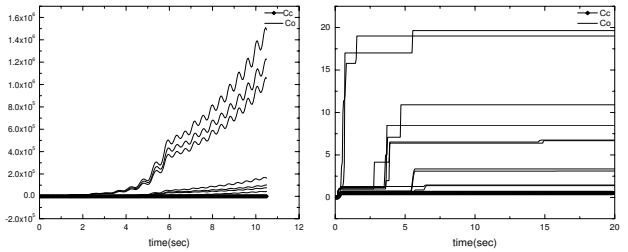

(a) (b)

Fig. 5. Controller cost with two different cost functions, with the plant $G_p(s) = 0.5/(s^2-0.35s+2)$

in Figs. 4-7, where column (a) shows the reference input $r(t)$, the reference model output $y_m(t)$, the plant response $y_p(t)$ and plant input $u(t)$ with the non-cost-detectable cost function($J_i(t) = -\rho + \int_0^t \Gamma_{spec}(\widetilde{r_i}(t), y(t), u(t))dt$), whereas column (b) shows the corresponding results with the cost-detectable cost function($J_i(t) = -\rho + \max_{\tau\in[0,t]} \frac{\|u\|_\tau^2 + \left\|\widetilde{e_i}\right\|_\tau^2}{\left\|\widetilde{r_i}\right\|_\tau^2}$). In Figs. 4(a), 7(a), $y_p(t)$ are both oscillatory divergent, and all candidate controllers are falsified in approximately 11 seconds. In Fig. 6(a), $y_p(t)$ is bounded, but the tracking error is rather large. In Figs. 4-7(b), the tracking error is considerably smaller. To clarify the difference between the above two cost functions, we decreased the dimension of controller set to $K_P = \{1, 50, 100\}$, $K_I = \{1, 50\}$, $K_D = \{0.2, 5, 15\}$. Fig. 5(a) shows the cost with the non-cost-detectable cost function on the plant $G_p(s) = 0.5/(s^2-0.35s+2)$, while Fig. 5(b) represents the corresponding cost with the cost-detectable cost function. In fig. 5, lines Cc and Co respectively stand for the costs of the selected controller and those of the non-selected ones. It is seen that the former cost function lacks the capability of selecting the "best" controller, or even discard the stabilizing controller. As expected, the stability and performance with the latter cost function are preserved.

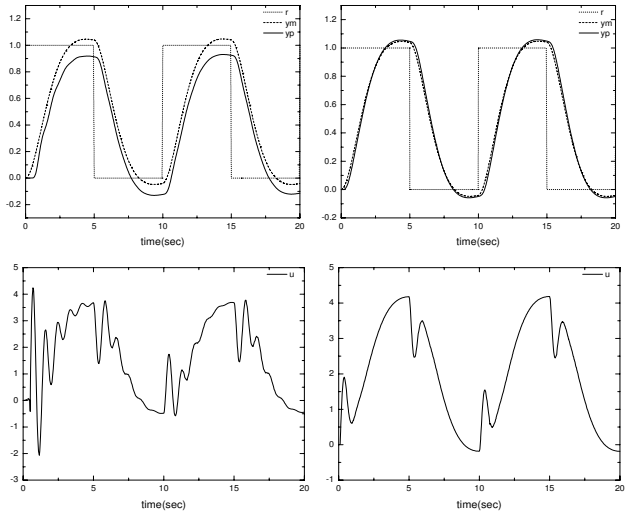

(a) (b)

Fig. 6. I/O data for the unstable oscillatory plant $G_p(s) = 0.5/(s^2 - 0.5s + 2)$ with two different cost functions

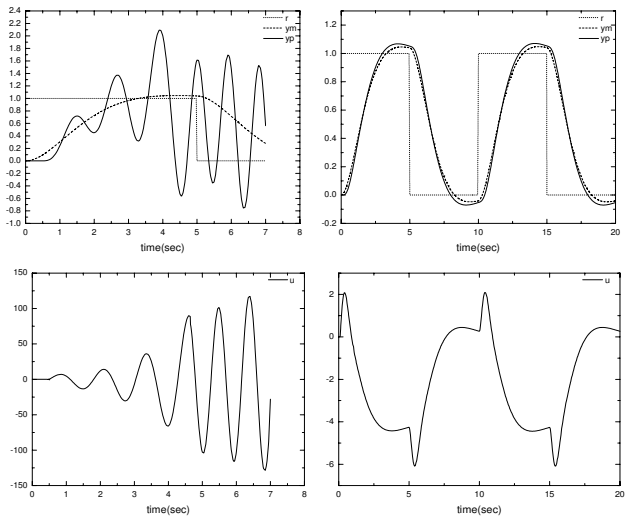

(a) (b)

Fig. 7. I/O data for the unstable nonoscillatory plant $G_p(s) = 0.5/(s^2 + 0.5s - 2)$ with two different cost functions

Moreover, compared with the results in Balakrishnan and Narendra [1994], we can conclude that the unfalsified control, under the feasibility assumption and with a properly designed cost function, can achieve similar, or even better response results.

Simulation 2 : Here we demonstrate the effectiveness of Neural networks combined with the unfalsified control. In this case, the controller set is set to be smaller to make results more obvious, e.g. $K_P = \{5, 50, 100\}$, $K_I = \{20, 30\}$, $K_D = \{0.2, 0.5, 1\}$. The cost function is the chosen to be the cost-detectable one. Other simulation parameters are the same as in the previous setting. Figs. 8, 10, 11 (b) show the simulation results with NN inserted to update the PID parameters of the controller being switched to the closed loop. Figs. 8, 10, 11 (a) show the simulations without NN.

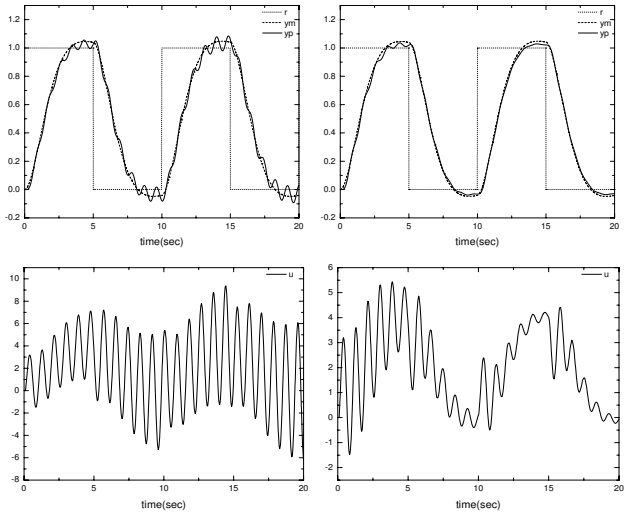

(a) (b)

Fig. 8. I/O data for the unstable oscillatory plant $G_p(s) = 0.5/(s^2 - 0.35s + 2)$. (a)without NN. (b) with NN

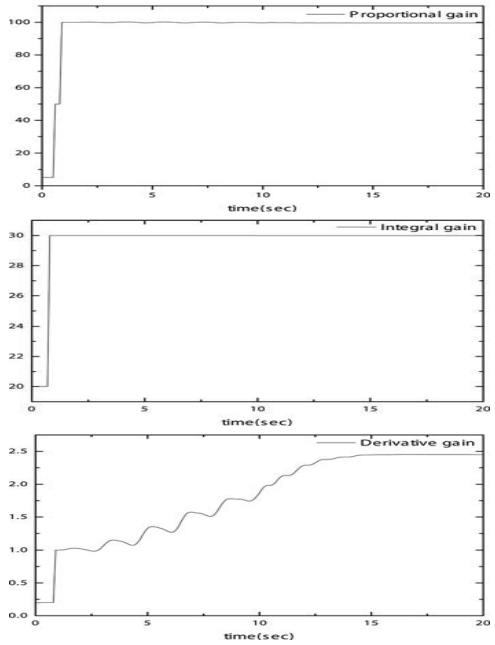

Fig. 9. PID gains with NN for the unstable oscillatory plant $G_p(s) = 0.5/(s^2 - 0.35s + 2)$.

By comparing Figs. 8, 10, 11 (b) with Figs. 8, 10, 11 (a), we can find that the combination of NN with the unfalsified control reduces the tracking error, and even stabilizes a divergent system, in the scenarios when the candidate controllers set is small, or does not match well with the actual plant, and all controllers in the controller set might be falsified. Fig. 9 shows the PID gains, which demonstrate the effect of NN.

Although the tracking error is increasing in the scenarios without NN (Figs. 8, 10, 11 (a)), as soon as stability is falsified by the switching algorithm (guaranteed by the cost-detectable cost function), the old controller will be switched out and replaced with an as-yet-unfalsified one. However, every new switching requires controller state

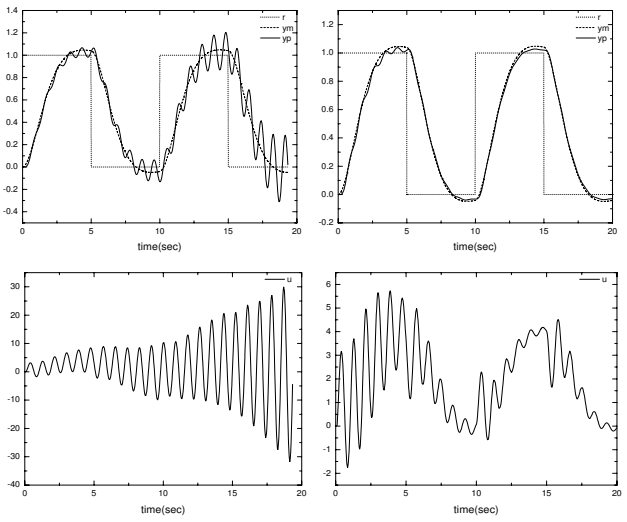

(a) (b)

Fig. 10. I/O data for the unstable oscillatory plant $G_p(s) = 0.5/(s^2 - 0.5s + 2)$. (a)without NN. (b) with NN

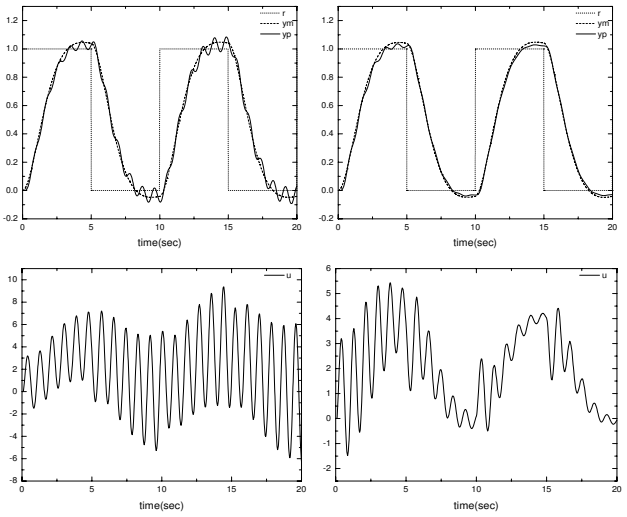

(a) (b)

Fig. 11. I/O data for the unstable nonoscillatory plant $G_p(s) = 0.5/(s^2 + 0.5s - 2)$. (a)without NN. (b) with NN

resetting in order to prevent undesirable oscillations in the output, which can be circumvented by the proper use of NN, as demonstrated.

6. CONCLUSION

New results for the combination of the neural networks with unfalsified control are presented. A cost-detectable switching cost is used and compared with a previously known, non-cost-detectable one. Nonlinear neural networks are used to update the parameters of the PID controller, which is switched according to the hysteresis switching algorithm. Simulations are conducted comparable to those in Balakrishnan and Narendra [1994], a well-known example on multi-model adaptive control, and the results demonstrate the validity of the proposed framework. Although improved performance can be obtained in principle by increasing the number of the candidate controllers, we focused here on the performance improvement given a fixed candidate set. This is important when one needs to work with a limited candidate set, due to the computational reasons, for example. The issue of how one can optimally utilize data for generating new candidate controllers on the fly remains an open question.

REFERENCES

J. Zhai and S. Fei. Multiple Model Adaptive Control Based on RBF Neural Network Dynamic Compensation. *ISNN*, 3:36–41, 2005.

E. D. Ferreira, and B. H. Krogh. Switching Controllers Based on Neural Network Estimates of Stability Regions and Controller Performance. *Automatica, Special Issue on Hybrid Systems*. 1999.

I. Skrjanc, S. Blazic, and D. Matko. Model-reference fuzzy adaptive control as a framework for nonlinear system control. *J. Intel. Robotic Systems*, pages 331–347, 2003.

J. Balakrishnan, and K.S.Narendra. Improving transient response of adaptive control systems using multiple models and switching. *IEEE Trans. Autom. Control*, vol. 39, pages 1861–1866, September 1994.

J. Balakrishnan, and K. S. Narendra. Adaptive control using multiple models. *IEEE Trans. Autom. Control*, vol. 42, February 1997.

J. P. Hespanha, D. Liberzon, and A. S. Morse. Hysteresis-based switching algorithms for supervisory control of uncertain systems. *Automatica*, 39:263–272, 2003.

M. Jun and M. G.Safonov. Automatic PID tuning: An application of unfalsified control. *Proc. IEEE CCA/CACSD*, vol. 2, pp. 328–333. HI, 1999.

Y. H. Lim and F. L. Lewis. *High-level feedback control with neural network. World Scientific*, Singapore, 1999.

M. Stefanovic, R. Wang, and M. G. Safonov. Stability and convergence in adaptive systems. *Proc. Amer. Contr. Conf.*, Boston, MA, 2004.

L. Chen and K. Narendra. Nonlinear adaptive control using neural networks and multiple models. *Automatica, special issue on neural network feedback control*, pages 1245–1255, 2001.

R. Wang, M. Stefanovic, M. G. Safonov. Unfalsified direct adaptive control using multiple controllers. *AIAA*, 2004.

M. Stefanovic and M. G.Safonov. Safe adaptive switching control: Stability and convergence. *IEEE Trans. Autom. Control*, To appear, 2007.

T. C. Tsao, and M. G. Safonov. The unfalsified control concept and learning. *IEEE Trans. Autom. Control*, pages 843–847, June 1997.

A. S. Morse, D. Q. Mayne and G. C. Goodwin. Applications of hysteresis switching in parameter adaptive control. *IEEE Trans. Autom. Control*, vol. 37, no. 9, pages 1343–1354, Sept. 1992.

C. Manuelli, S.G. Cheong, E. Mosca and M. G. Safonov. Stability of Unfalsified Adaptive Control with Non SCLI controllers and Related Performance Under Different Prior Knowledge. *Euro. Contr. Conf.*, 2007, Kos, Greece.

A. Dehghani, B. D. O. Anderson and A. Lanzon, "Unfalsified Adaptive Control: A New Controller Implementation and Some Remarks", *European Control Conference*, 2007, Kos, Greece.